A.E.Ü., Vol. 23
1969, Part 4

AN IMPROVED HORN FEED WITH TWO MODES FOR SHALLOW PARABOLOID ANTENNAS

VERBESSERTER HORNERREGER MIT ZWEI WELLENTYPEN FUR FLACHE PARABOLANTENNEN

Research Institute for High-Frequency Physics, Werthoven
Mitteilung aus dem Forschungsinstitut fur Hochfrequenz-
physik, Werthoven

by
Elfriede Ludwig, Gunter Ries, and Eberhard Zocher

Translated by the Center for Foreign Technology
Pasadena, California, on 10 Sept 1969

Prepared for and issued by the Jet Propulsion Laboratory,
California Institute of Technology, Pasadena, Calif.
under NASA contract NAS 7-100.

AN IMPROVED FORN FEED WITH TWO MODES FOR SHALLOW PARABOLOID ANTENNAS

by

ELFRIEDE LUDWIG, GUNTER RIES, and EBERHARD ZOCHER*

Report from the Forschungsinstitut fur Hochfrequenzphyzik (Research Institute for High-Frequency Physics), Werthoven.

(A.E.U 23 (1969), Part 4. 209-215; entered on August 26, 1968)

DK 621.396.677.73

1. Introduction

Parabolic reflector antennas with proportionately large apertures are used for various tasks that require high-antenna gain. In these cases, the extent to which the available aperture can be used depends on the feed system. For rotation-symmetrical refelctor systems with a ratio of focal point distance to diameter $F:D>1$, e.g., Cassegrain systems, the theoretical antenna efficiency is maximally $\eta=0.74$ for simple, conical horn feeds with H_{11} (see below) and $\eta=0.76$ for simple pyramidal horn feeds with H_{01} excitation (Ref 1).The values obtained in practice are around $\eta=0.6$. A higher degree of antenna efficiency, which is of greatest interest for large reflectors in view of their great cost, can be achieved by improving the feed. Several means of accomplishing this are known, which can be explained on the basis of the field distribution around the reflector focal point.

Assuming a reflector system with $F:D>1$, with a plane wave entering the focal plane in an axial direction, the well-known Airy field distribution is yielded from the A_1 function as a result of diffraction, as shown in Fig. 1. The middle zone contains 83.3% of the total energy; the first, second, and third annular zones contain 7.2%, 2.8%, and 1.45%. An antenna efficiency $\eta=1$ can be attained theoretically only with an appropriate feed system, which accepts the entire energy that passes through the focal plane. For reasons of reciprocity, there is a parallel consideration in the case of transmission. Here, an antenna efficiency $\eta=1$ is yielded only with constant illumination of the reflector mechanism without halation of the reflector rim, i.e., for a sector-shaped feed conficguation. The required illumination function for a horn feed with such a configuration again is the Airy distribution sketched in the figure (Ref. 2). This zone-shaped field

* Dipl.-Phys. E. LUDWIG, Dr. G. Ries, and Dipl.-Eng. E. ZOCHER, at the Forschungs Institute fur Hochfrequenzphyzik, 5321 Werthoven, Konigstrasse 2.

distribution is maintained in its basic form even for reflector systems with $F:D<1$, but in that case, additional cross-polarization components appear.

The illumination function of simple, classic horn feeds, articularly the constant or nearly constant illumination in the E-plane, makes possible only an unsatisfactory approximation of the Airy distribution. Some improvement can be achieved by graduating the illumination of the E-plane, e.g., per Ref. 3. More advantageous are more complex feed systems composed of several inividual feeds, which also utilize the annular zones of the Airy distribution but, in turn, require more complicated feed systems (Refs. 4,5). Another possibility is to approximate the Airy distribution using only one horn feed with an appropriatly large aperture, by means of superimposing several modes of the proper amplitude and phase in the feeding waveguide (Refs. 6,7). The correct excitation of the individual modes is a problem here, but such a horn feed with only two modes, referred to for short as an improved horn feed, is relatively simple to construct (Refs. 8,9,10).

In the following we shall examine, with respect to usability in a Cassegrain antenna with $F:D=1.27$, what improvements can be achieved with a conical, improved horn feed vs the classic horn with H_{11} excitation. In addition, an excitation system for this horn will be experimentally investigated.

2. Field-intensity ratio and aperture diameter

Several modes exist in the waveguide on the feed side of the horn, whose propagation in the horn cone can safely be assumed with a sufficiently small cone-aperture angle. In the case of the transmitter, the maximum antenna gain, or in the case of the receiver, the maximum ratio between antenna gain and antenna noise temperature -- can be assumed as criterion for the determination of the optimal field-intensity ratio of these modes in the horn mechanism and of the optimum aperture diameter of the horn. Since the antenna noise temperature depends of the elevation of the antenna and is therefore difficult to obtain, the following theoretical considerations will be based on the requirement for a maximum antenna gain.

The antenna gain for polarization in the x-direction is generally given by the ratio of the output in the axial direction per solid unit to the total radiated output of the antenna -- in this case, therefore, of the horn mechanism (Ref. 11):

$$G_x = \frac{\dfrac{1}{2Z_0}\left|\dfrac{1}{\lambda_0}\displaystyle\int_0^{D/2}\int_0^{2\pi} E_{Ax}\, R\, dR\, d\Phi\right|^2}{\dfrac{1}{4\pi}\displaystyle\int_0^{d/2}\int_0^{2\pi} \mathrm{Re}\left(\dfrac{E_t H_t^*}{2}\right) r\, dr\, d\varphi}. \qquad (1)$$

where E_{Ax} is the x-component of the field intensity of the antenna mechanism, E_t and H_t are the tangential field intensity components in the horn aperture, Z_0 is the wave resistance of free space, and λ_0 is the free space wavelength. The meaning of the remaining magnitudes is given by the coordinate system in Fig. 2. In the case of an ideal parabolic reflector in the remote radiation field of the horn feed taking under consideration simple paraboloid relations and the orthogonality of the waveguide modes it follows after a few calculations that:

$$G_z = \left(\frac{\pi D}{\lambda_0}\right)^2 \frac{1}{\pi} \cot^2 \frac{\vartheta_R}{2} \times$$
$$\times \frac{\left|\sum_\nu \int_0^{\vartheta_R} \int_0^{2\pi} (g_{\nu\vartheta} \cos\varphi - g_{\nu\varphi} \sin\varphi) \tan\frac{\vartheta}{2}\, d\vartheta\, d\varphi\right|^2}{\sum_\nu \frac{Z_0}{Z_{t\nu}} \int_0^{d/2} \int_0^{2\pi} |E_{t\nu}|^2\, r\, dr\, d\varphi}. \quad (2)$$

where summation is made over all excited waveguide modes, and g_ν or $Z_{t\nu}$ indicate the field-intensity diagram factors and the transverse field wave resistances of these modes.

The first factor in Eq. (2) corresponds to the maximum possible theoretical antenna gain; the remaining expression to the total efficiency η, obtained by multiplying the feed and aperture efficiencies,

$$\eta = \frac{1}{\pi} \cot^2 \frac{\vartheta_R}{2} \times$$
$$\times \frac{\left|\sum_\nu \int_0^{\vartheta_R} \int_0^{2\pi} (g_{\nu\vartheta} \cos\varphi - g_{\nu\varphi} \sin\varphi) \tan\frac{\vartheta}{2}\, d\vartheta\, d\varphi\right|^2}{\sum_\nu \frac{Z_0}{Z_{t\nu}} \int_0^{d/2} \int_0^{2\pi} |E_{t\nu}|^2\, r\, dr\, d\varphi}, \quad (3)$$

which is to be optimized below.

In the improved conical horn feed, the E_{11} mode is excited at the horn axis in addition to the H_{11} basic mode, both with the same polarization. The effects of the E_{11} mode on the exciter diagram, the lack of effect in the H -plane, and the expansion of the principal lobe in the E-plane with simultaneous reduction of the minor lobes are discussed in detail elsewhere (Ref. 9).

If we neg;ect the minor quadratic phase errors at small aperture angles of the horn cone as well as the reflections in the horn mechnism, then, according to Ref. 11, the following applies for the field-intensity diagram factors of these two modes:

H_{11} mode:

$$g_{H_{11}\vartheta} = E_{0H_{11}} \frac{d}{2} g'_{H_{11}\vartheta}(\vartheta) \cos\varphi \quad (4a)$$

with
$$g'_{H_{11}\vartheta}(\vartheta) = \frac{\pi}{2}\frac{d}{2}\left[1 + \sqrt{1 - \left(\frac{1.84}{\pi}\frac{\lambda_0}{d}\right)^2} \cos\vartheta\right] \frac{J_1\left(\pi \frac{d}{\lambda_0} \sin\vartheta\right)}{\pi \frac{d}{\lambda_0} \sin\vartheta},$$

$$g_{H_{11}\varphi} = -E_{0H_{11}} \frac{d}{2} g'_{H_{11}\varphi}(\vartheta) \sin\varphi \quad (4b)$$

with
$$g'_{H_{11}\varphi}(\vartheta) = \frac{\pi}{2}\frac{d}{2}\left[\sqrt{1 - \left(\frac{1.84}{\pi}\frac{\lambda_0}{d}\right)^2} + \cos\vartheta\right] \frac{J'_1\left(\pi \frac{d}{\lambda_0} \sin\vartheta\right)}{1 - \left(\frac{\pi}{1.84}\frac{d}{\lambda_0} \sin\vartheta\right)^2};$$

E_{11} mode:

$$g_{E_{11}\vartheta} = -E_{0E_{11}} \frac{d}{2} g'_{E_{11}\vartheta}(\vartheta) \cos\varphi \quad (5a)$$

with

$$g_{E_{11}\vartheta}(\vartheta)=\frac{1}{2\sin\vartheta}\left[1+\frac{\cos\vartheta}{\sqrt{1-\left(\frac{3{,}83}{\pi}\frac{\lambda_0}{d}\right)^2}}\right]\frac{J_1\left(\pi\frac{d}{\lambda_0}\sin\vartheta\right)}{\frac{1}{\left(\frac{\pi}{3{,}83}\frac{d}{\lambda_0}\sin\vartheta\right)^2}-1}, \tag{5b}$$

$$g_{E_{11}r}=0,$$

$$g'_{E_{11}r}(\vartheta)=0.$$

For the output expressions of the two modes in the denominator of (3), the following applies:

H_{11} mode:

$$\frac{Z_0}{Z_{tH_{11}}}\int_0^{d/2}\int_0^{2\pi}|E_{tH_{11}}|^2 r\,dr\,d\varphi=\frac{\pi}{2}\frac{d^2}{4}2{,}39\sqrt{1-\left(\frac{1{,}84}{\pi}\frac{\lambda_0}{d}\right)^2}\,|E_{0H_{11}}|^2, \tag{6}$$

E_{11} mode:

$$\frac{Z_0}{Z_{tE_{11}}}\int_0^{d/2}\int_0^{2\pi}|E_{tE_{11}}|^2 r\,dr\,d\varphi=\frac{\pi}{2}\frac{d^2}{4}\frac{1}{\sqrt{1-\left(\frac{3{,}83}{\pi}\frac{\lambda_0}{d}\right)^2}}\,|E_{0E_{11}}|^2. \tag{7}$$

In the above equations, $E_{OE_{11}}$ and $E_{OH_{11}}$ refer to the rim field intensities of the E_{11} and H_{11} modes for $\phi=0$, whose ratio shall be designated as field-intensity ratio ε for short. From Eq. (3), with (4) to (7), it follows that

$$\eta=2\cot^2\frac{\vartheta_R}{2}\cdot\frac{\left|\int_0^{\vartheta_R}(g_{H_{11}\vartheta}-\varepsilon g_{E_{11}\vartheta}+g_{H_{11}r})\tan\frac{\vartheta}{2}\,d\vartheta\right|^2}{2{,}38\sqrt{1-\left(\frac{1{,}84}{\pi}\frac{\lambda_0}{d}\right)^2}+|\varepsilon|^2\frac{1}{\sqrt{1-\left(\frac{3{,}83}{\pi}\frac{\lambda_0}{d}\right)^2}}}. \tag{8}$$

Equation (8) yields the maximum increase in η as compared with the case of the classic horn feed with $\varepsilon=0$ for negative true field-intensity ratios ε. Numerical results, i.e., the efficiency as a function of the diameter of the horn aperture for various field-intensity ratios, are shown in Fig. 3. The junction curve of the efficiency maxima is also entered, with the field intensity ratio as a parameter. This results in a maximum efficiency of about 82% for an optimally dimensioned improved horn feed ($\varepsilon=-0.6$, $d/\lambda\cdot D/F=2.38$), that is, an increase of about 8% over the optimum classic horn ($\varepsilon=0$, $d/\lambda_0\cdot D/F=2.05$). Minor deviations from the optimum field-intensity ratio and optimum aperture diameter are not critical because of the relatively shallow absolute maximum.

In the planned standardization of the horn-aperture diameter, the curves shown are independent of the $F:D$ ratio of the reflector systems as long as $F:D$ is sufficiently large.. Strictly speaking, this assumption applies only for $F;D\to\infty$, but in practwce even for $F:D>1$, so that the curves computed here are valid with good approximation for a Cassegrain antenna with $F:D=1.27$ in the entire region $F:D>1$.

The increase in the antenna efficiency can be explained by the improved utilization of the energy flowing through the inner zone of the Airy distribution. Figure 4 shows the transverse usable polarization field intensity E_x in the aperture of the improved horn feed, with reference to the field intensity in the center of the aperture E_0, and, for comparison, this field intensity in the classic horn with the same aperture diameter. The corresponding region of the Airy distribution is indicated in both cases. Accordingly, a considerably better adaptation of the E_x aperture illumination to the middle zone of the Airy distribution results for the improved horn feed than for the classic horn Furthermore, the cross-polarization field intensity E_y in the aperture is less in the case of the improved horn feed, as can be seen in Fig. 5, in which the E_y- aperture illuminations of the two horns are represented.

Figure 6 shows the configurations of the improved horn feed computed according to Eqs. (4) and (6). For comparison, the E-plane configuration of a classic horn with the same aperture diameter is entered; the H-plane configurations of the two horns are identical because of Eq. (5b). The advantage of these feed configurations is obvious. In the E-plane and H-plane, practically identical reflector illuminations result, with a drop at the rim of 11 dB; in addition, the minor lobes in the E-plane are considerably reduced. Because of the two practically identical configurations in the principal planes, the improved horn feed is also well suited as a feed in the case of circular polarization.

3. Producing the field-intensity ratio

There are several conceivable methods for exciting the optimum field-intensity ratio determined in the preceding section. The field conversion with a round aperture and a spiral-shaped increase in diameter in the feeding waveguide have already been discussed (Refs. 12, 13). Here, we shall examine the field conversion with a conical transition, which appears advantageous in view of the maximum transferrable output in greater detail.

The transition shown in Fig. 7 is fed across the feeding waveguide with diameter d'' with the usual H_{11} mode, polarized, for example, in the x-direction. To fulfill the rim conditions, then, a mixture of all modes symmetrical to the x-direction will be produced at the cone, with only the H_{11} and E_{11} modes able to propagate in the adjacent waveguide with diameter d'. The diameter d' was selected so that it is above the critical diameter of the E_{11} mode but below the perturbing H_{31} mode. The absolute amount of the field-intensity ratio $|\varepsilon'|$ can be varied by changing the cone angle α'; the phase of the field-intensity ratio is not of immediate interest.

Since a mathematical treatment of the problem did not appear to justify the expense involved in the numerical evaluation, corresponding experimental investigations were carried out. The field-intensity ratio was determined using an appropriate ranging circuit connected in series with the conical transition. Some difficulty was caused by reflections at the terminal of the circuit, which could not be made ideally absorbing for both modes, but the errors caused by this could be eliminated by averaging at a different absorber position.

Figure 8 shows the results, i.e., the field-intensity ratio as a function of wavelength for various cone angles α'. The upper and lower limits required by the H_{31} and E_{11} critical wavelengths constrain the bandwidth to about 11%; however, because of the phase error in the aperture of the improved horn feed to be discussed later, only about 2% could be used. Within such a narrow range, the frequency dependence of the field-intensity ratio is minimal.

The H_{11} wave reflected into the feed waveguide has an unfavorable effect on the adaptability of the transition. Table 1 presents measured input standing-wave ratios.

The field-intensity ratio produced by the conical transition changes in the connected horn cone. Under the assumption of a small cone angle α', i.e., with negligibly small additional field conversion in the cone, a constant output in both modes can be counted on. With this assumption, Eqs. (6) and (7) yield, for the field-intensity ratio in the feed mechanism ε: Hereafter, $\varepsilon > \varepsilon'$ shall be valid for $d > d'$; the exact dependence is shown in Fig. 9. The required field-intensity ratios $|\varepsilon| < 0.6$ for the optimally dimensioned improved horn feed can then always be attained with the conical transition examined here at a relatively small cone angle and, thus, at a small standing-wave ratio of the conical transition.

4. Measured configurations

The configurations obtainable with an improved horn feed are known from Ref. 9. We shall therefore discuss here only briefly the configuration of an optimally dimensioned improved horn feed based on the preceding investigations, with particular emphasis on the wide-band aspect. The measurements according to Fig. 7 are:

d= 102mm, d'=42.7 mm, d''=22.8 mm, α'=65 deg, f_0=9.15 GHz

On the one hand, the horn cone angle had to be as small as possible to minimize undesirable additional field conversion in the horn cone and quadratic phase errors in the horn aperture, but on the other hand, the horn cone had to be as short as possible in order to obtain an in-phase superimposition of the two modes under wide-band conditions in the horn aperture. The value α=12 deg was selected as a compromise. The in-phase superimposition of the two modes in the aperture at midband frequencies was regulated by making a corresponding change in the interval l'.

Fig. 10 shows the measured configurations in the E - and H-planes. For comparison, the configurations computed according to Eqs. (4) and (5) are entered, as well as those of a classic horn with the same aperture angle and diameter. The minor differences must have been caused by the effects not considered in the computation, such as reflections and field conversion in the cone, phase errors in the aperture, and rim flow effects. The improvements in the E -plane with respect to the classic horn indicated in Fig. 6 are obvious. Up to the peripheral ray angle, the configurations in the two planes are practically identical at about 13 dB. The measured cross-polarization field intensity in all regions was more than 35 dB below the effective polarization field intensity in the direction of the main radiation.

The narrow-band properties of the improved horn feed can be seen in Figs. 11 and 12. According to these, the configuration changes in the *E*-plane remain small within a range of ±1% about the middle frequency, but at stronger frequency deviations, e.g., even at ±2.5%, the changes are considerable. These distortions in the configurations are caused essentially by the out-of-phase superimposition of the two modes in the feed mechanism and only to a small degree by the low frequency dependence of the field conversion on the conical transition. In the *H*-plane, where the E_{11} mode has no effect, the wide-band effect of the classic horn feed is maintained.

5. Conclusions

The theoretical investigations discussed here have shown that, in the optimum case, an increase in the antenna effectiveness of some 8% to about 82% can be achieved by the supplemental use of the E_{11} mode in the conical, improved horn feed as compared to the classic horn feed. The energy in the middle Airy zone of the reflector is used almost fully, and a considerable further increase of the antenna effectiveness can be achieved only by utilizing the outer Airy rings, with a correspondingly more expensive feed (Ref. 5).

The required ratio of E_{11} to H_{11} modes in the feed aperture can be produced without great expense by the conical transition in the feed circuit investigated here, so that an improved horn feed can be constructed relatively easily in spite of the desired improvements. As a result of the narrow-band in-phase superimposition of the E_{11} and H_{11} modes, the broad bandwidth of the classic horn feed is sacrificed; however, within a frequency range of 2%, the changes in configuration are acceptably small.

The authors thank Dr. W. RUPPEL for his sponsorship of this work, as well as the "Forschungsinstitut fur Funk und Mathematik" for making available the TR4 computer for the numerical evaluation.

REFERENCES

1. MILNE, K. and RAAB, A.R., Optimum illumination tapers for four-horn and five-horn monopulse aerial systems. IEEE Conference, "Design and Construction of Large Steerable Aerials". London, June 1966.

2. RUZE, J., Circular aperture synthesis, Transact. Inst. Elect. Electron. Enggrs. AP-1? (1964) 691-694.

3. PEACE, G.M. and SCHWARTZ, E.E., Amplitude compensated horn antenna, Microwave J., 7, (1964) H, 2, 66-68.

4. JASIK, H. and BRESLER, A.D., A low impulse noise feed system for large parabolic reflector antennas, In E.C. JORDAN (ed.) "Electromagnetic theory and antennas, Vol. 2". Pergamon Press, London, 1963, 8, 1167-1174.

5. KOCH, G.F., A feed for noise-free paraboloid antennas and other possibilities for obtaining an A_1 illumination. Nachrichtentech. Z., 18, (1965) 1-6.

6. MINNETT, H., and THOMAS, B. MACA, Synthesis of improved feeds for large circular paraboloids, IEE Conference "Design and Construction of Large Steerable Aerials". London, June 1966.

7. LUDWIG, A.C., Radiation pattern synthesis for circular aperture horn antennas. Transact. Inst. Elect. Electron. Engrs. AP-14, (1966), 431-440.

8. POTTER, P.D. and LUDWIG, A.C., Beamshaping by use of higher order modes in conical horns, NEREM Record. 1963, 8, 92-93.

9. POTTER, P.D., A new horn antenna with suppressed sidelobes and equal beamwidths., Microwave J., 6 (1963) 11, 6, 74-78.

10. JENSEN, P.A., Low noise multimode Cassegrain monopulse feed with polarization diversity. NEREM Record. 1963, 8, 94-95.

11. SILVER, S., Microwave antenna theory and design. McGraw Hill Book Co., New York, 1949.

12. YEH, C. Excitation of higher order modes by a step discontinuity of circular waveguides, Jet Prop. Lab., Pasadena, Tech Rep. 32-496, Feb 1964.

13. NAGELBERG, E.R. and SCHEFER, J. Mode conversion in circular waveguides. Bell Syst. tech. J. 44 (1965) 1327-1338.

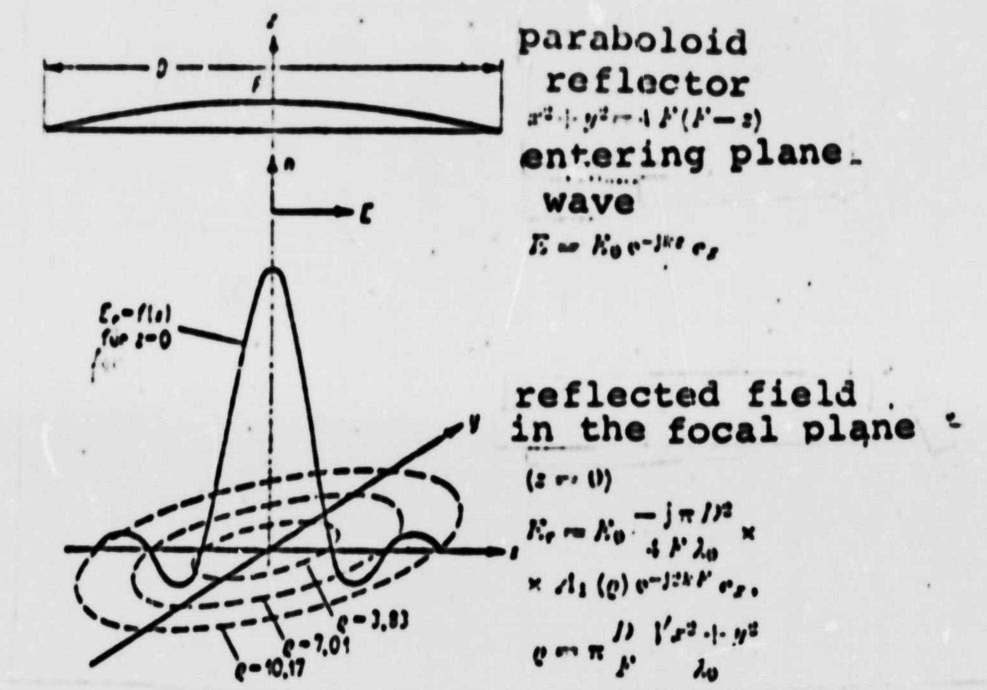

Fig. 1. Field distribution in the focal plane of a paraboloid reflector with $F/D \gg 1$.

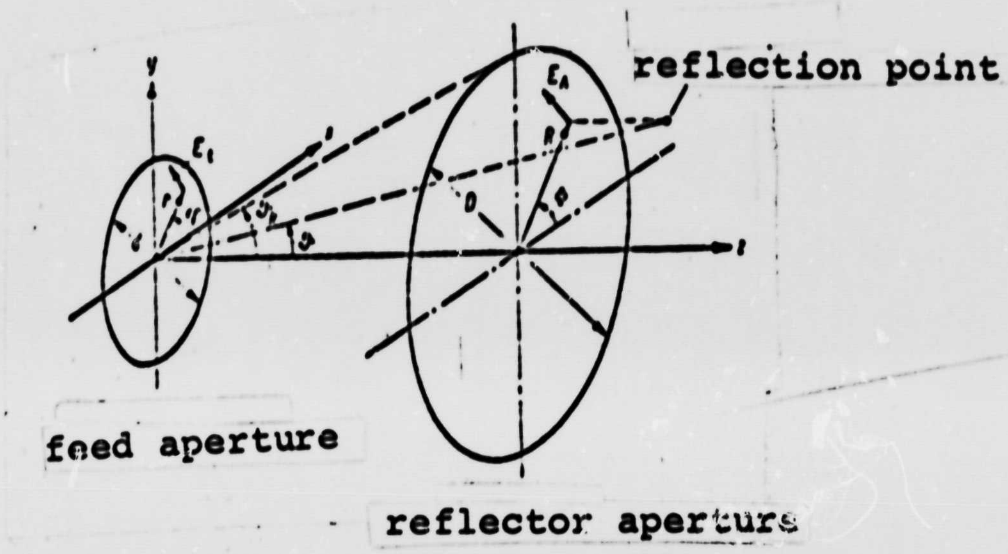

Fig. 2. Coordinate system

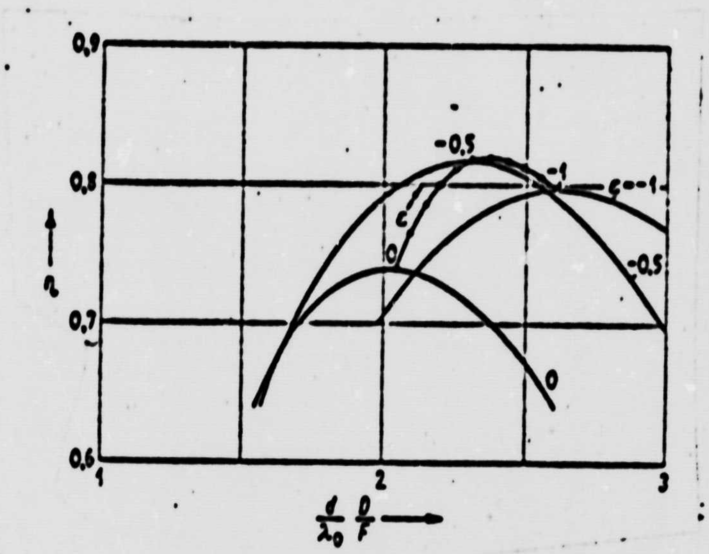

Fig. 3. Antenna efficiency as a function of aperture diameter for an improved horn feed at various field intensity ratios.

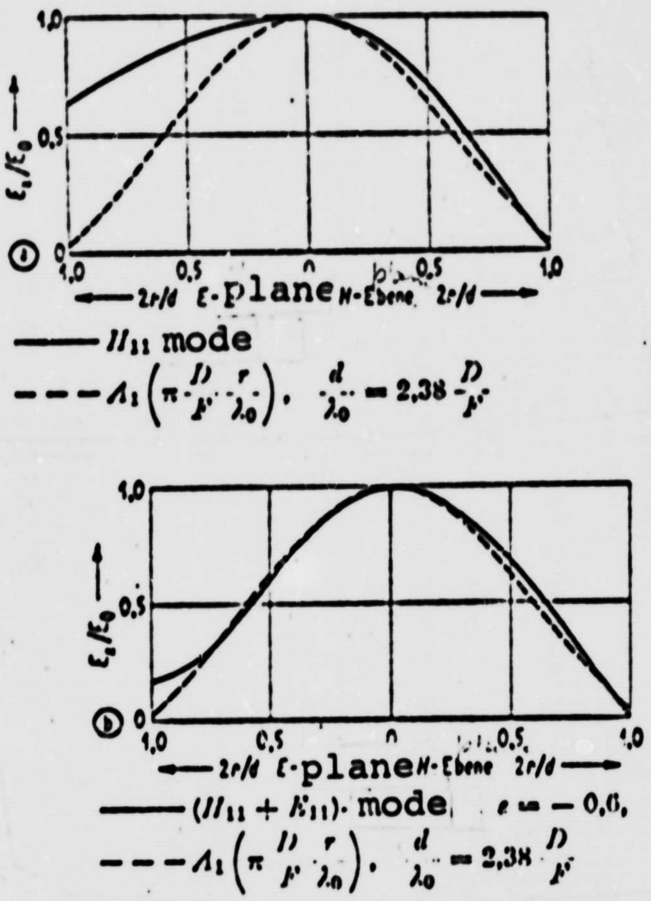

Fig. 4. Aperture illumination of the improved horn feed (b) compared with aperture illumination of the classic horn(a).

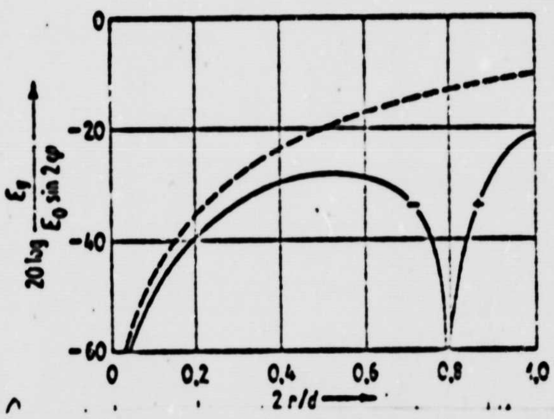

Fig. 5. Cross-polarization in the aperture of the improved horn feed.

- - - H_{11}- mode

—— $(H_{11} + E_{11})$- mode $\varepsilon = -0{,}6$.

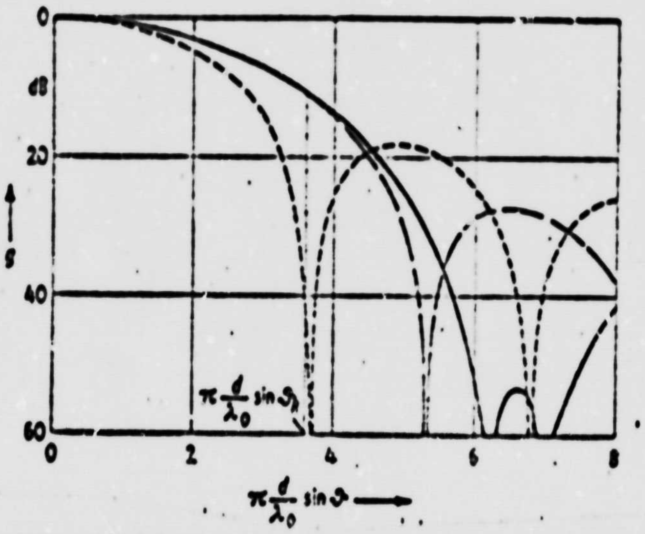

Fig. 6. Configuration of the improved horn feed with optimum field intensity ratio.

— — H-Horn, plane
——— E-Horn, $c = -0.6$,
- - - E-Horn, $c = 0$.

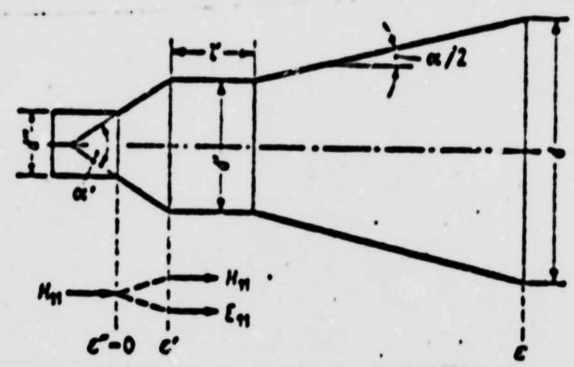

Fig. 7. Horn with conical transition for field conversion; $d''/d' = 0.535$.

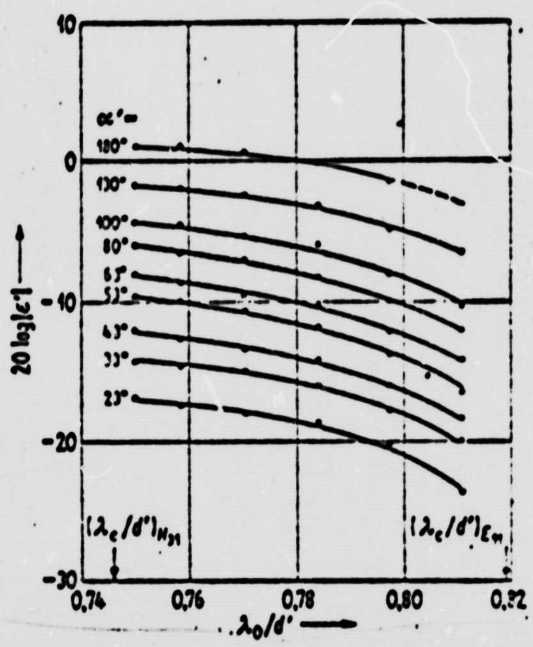

Fig. 8. Field conversion of the conical transition with $d''/d' = 0.535$.

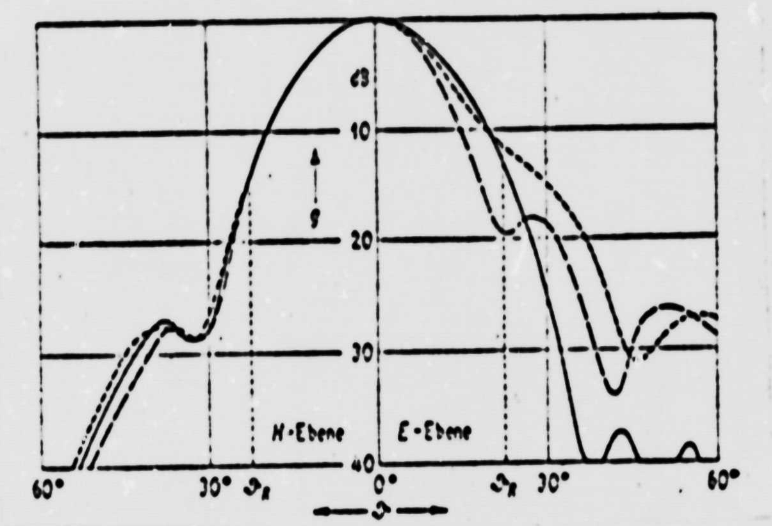

Fig. 12. Configuration deformation of the improved horn feed at frequency changes of ±2.5%.

——— f_0 = 9,15 GHz.
– – – f = 8,92 GHz.
— — f = 9,38 GHz.

Table 1. Pulsation factor of the conical transitio transition ($d''/d' = 0.535$).

α'	s		
	$\lambda_0/d' = 0{,}8$	$\lambda_0/d' = 0{,}77$	$\lambda_0/d' = 0{,}75$
180°	2,2	1,8	1,45
70°	1,5	1,25	1,15